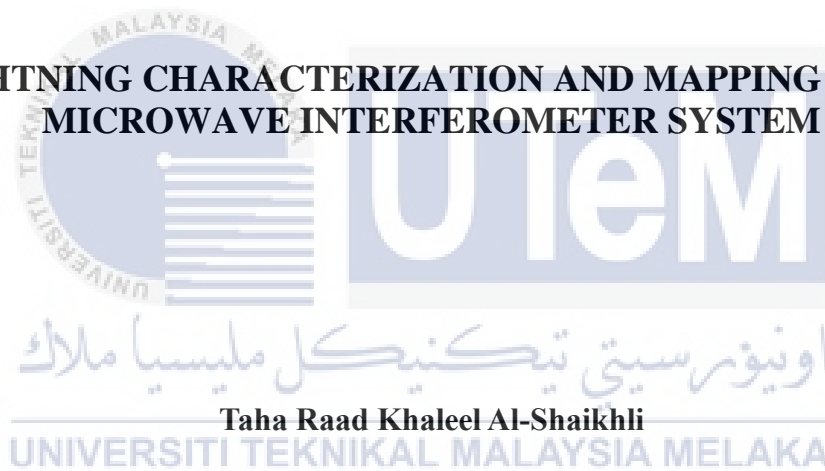




Faculty of Electronics and Computer Engineering

**LIGHTNING CHARACTERIZATION AND MAPPING USING
MICROWAVE INTERFEROMETER SYSTEM**



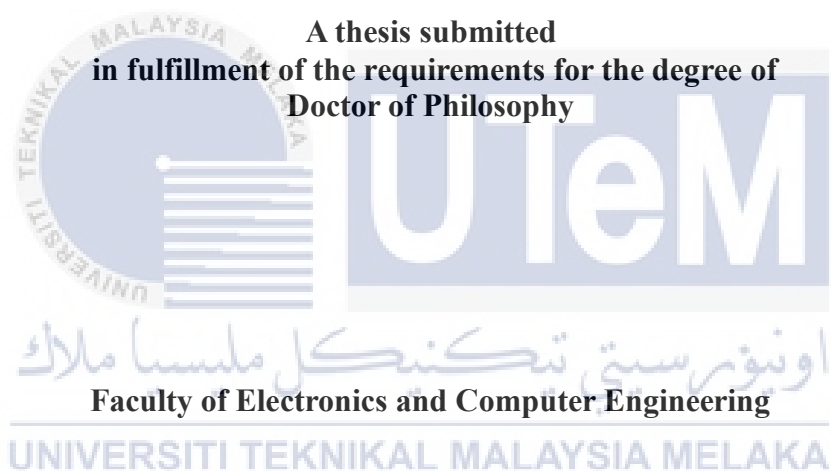
Taha Raad Khaleel Al-Shaikhli

Doctor of Philosophy

2021

**LIGHTNING CHARACTERIZATION AND MAPPING USING MICROWAVE
INTERFEROMETER SYSTEM**

TAHA RAAD KHALEEL AL-SHAIKHLI

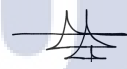


UNIVERSITI TEKNIKAL MALAYSIA MELAKA

2021

DECLARATION

I declare that this thesis entitled “Lightning Characterization and Mapping using Microwave Interferometer System” is the result of my own research except as cited in the references. The thesis has not been accepted for any degree and is not concurrently submitted in candidature of any other degree.

 Signature : 

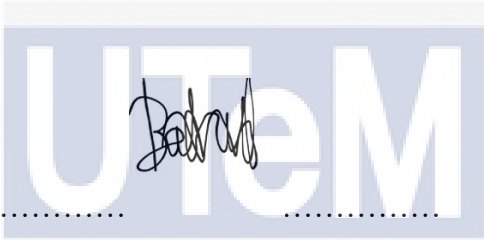
Name : Taha Raad Khaleel Al-Shaikhli

Date : 25/9/2021 

UNIVERSITI TEKNIKAL MALAYSIA MELAKA

APPROVAL

I hereby declare that I have read this thesis and in my opinion this thesis is sufficient in terms of scope and quality for the award of Doctor of Philosophy.

 
Signature :
Supervisor Name : Professor Dr. Badrul Hisham Bin Ahmad
Date :25/9/2021.....
UNIVERSITI TEKNIKAL MALAYSIA MELAKA

DEDICATION

First and foremost, Alhamdulillah Almighty for all the blessings of health, wisdom and patience to overcome all the difficulties that I faced in my PhD journey.

I would like to dedicate these years of hard work and absence to the spirits of my mother Sahar Saadi, my sisters Raghda and Ayat, and for my fabulous father Raad Khaleel Al-Shaikhli for all his help, supporting and praying to complete my study.

Special thanks to my life partner, my lovely wife Mays Yasir who supported me and gave me psychological and moral boost support to complete my study and her patience during past years. For my princes Raghda and Anas. As well as my brother Khaleel and Baji Eman. Thanks for my father in-law Yasir and my mother in-law Yusra, Abdullah and Elaff for their supports and prays to me.

UNIVERSITI TEKNIKAL MALAYSIA MELAKA

ABSTRACT

A lightning flash starts with the very first process called electron avalanche followed by streamer and leader. A leader is suggested to radiate intense electromagnetic fields below medium frequency (MF) bands while streamers are suggested to radiate intense very high frequency (VHF) electromagnetic fields. On the other hand, simulation results suggested that electron avalanches radiate strong microwave electromagnetic fields at around 1 GHz. In this thesis, a microwave interferometer system has been developed, fabricated, and deployed with the aim to evaluate the temporal and spatial (2D mapping) characteristics of electron avalanches development during narrow bipolar event (NBE) discharges. So far, nothing has been published about microwave interferometer system with the purpose to map lightning microwave radiation. As the streamer is preceded by electron avalanches, detecting microwave radiation before the onset of VHF radiation could be used as a method to prove that electron avalanches radiate strong microwave radiation. In order to establish a microwave interferometer system, three finite-length capacitive antennas with resonance frequency around 1 GHz, low noise amplifier (LNA) operating between 0.9 and 1.2 GHz, bandpass filter (BPF) operating between 0.95 and 1.05 GHz have been designed and fabricated. Microwave radiations associated with 98 NBEs have been recorded and analysed. Out of 98 NBEs, only 18 high amplitude and low noise NBEs were selected with 17 +NBEs and one -NBE. About 11 from 18 microwave radiations have been detected earlier than VHF and NBEs onset time with average lead time of 211.55 ± 82.49 ns. This is a strong indication of electron avalanches detected around 200 ns before the streamer formation. Moreover, clear bipolar pulses with duration less than 50 μ s have been observed during the initial stage (IS) of the main burst. It can be suggested that electron avalanches process behave impulsively before the propagating streamers formed. Furthermore, three NBEs with associated microwave radiations have been mapped where the azimuth and elevation angles can be determined. The maps proved that all three NBEs were the result of fast positive breakdown where the electron avalanches (microwave) propagated upward while the positive streamers propagated downward.

PENCIRIAN DAN PEMETAAN KILAT MENGGUNAKAN SISTEM INTERFEROMETER GELOMBANG MIKRO

ABSTRAK

Sebuah kilat bermula dengan proses pertama yang dikenali sebagai longsor elektron diikuti oleh pengalir dan pemimpin. Pemimpin memancarkan medan elektromagnetik yang kuat di bawah jalur frekuensi sederhana (MF) sementara pengalir memancarkan medan elektromagnetik frekuensi sangat tinggi (VHF). Sebaliknya, hasil simulasi menunjukkan bahawa longsor elektron memancarkan medan elektromagnetik gelombang mikro yang kuat pada sekitar 1 GHz. Dalam tesis ini, sistem interferometer gelombang mikro telah dikembangkan, dibuat, dan digunakan dengan tujuan untuk menilai ciri-ciri masa dan ruang (pemetaan 2D) pengembangan longsor elektron semasa pelepasan kejadian dwipolar sempit (NBE). Sejauh ini, belum ada yang diterbitkan mengenai sistem interferometer gelombang mikro dengan tujuan untuk memetakan sinaran gelombang mikro kilat. Oleh kerana pengalir didahului oleh longsor elektron, mengesan radiasi gelombang mikro sebelum bermulanya radiasi VHF dapat digunakan sebagai kaedah untuk membuktikan bahawa longsor elektron memancarkan radiasi gelombang mikro yang kuat. Bagi mewujudkan sistem interferometer gelombang mikro, tiga antena kapasitif dengan frekuensi resonans sekitar 1 GHz, penguat kebisingan rendah (LNA) yang beroperasi antara 0.9 dan 1.2 GHz, penapis jalur lebar (BPF) yang beroperasi antara 0.95 dan 1.05 GHz telah dirancang dan dibuat. Sinaran gelombang mikro yang berkaitan dengan 98 NBE telah direkodkan dan dianalisis. Daripada 98 NBE, hanya 18 NBE dengan amplitud tinggi dan kebisingan rendah yang dipilih dengan 17 +NBE dan satu -NBE. Kira-kira 11 dari 18 radiasi gelombang mikro telah dikesan lebih awal daripada masa permulaan VHF dan NBE dengan purata masa petunjuk 211.55 ± 82.49 ns. Ini adalah petunjuk kuat berkaitan longsor elektron yang dikesan sekitar 200 ns sebelum pembentukan pengalir. Lebih-lebih lagi, denyutan dwipolar yang jelas dengan jangka masa kurang dari 50 μ s telah diperhatikan semasa peringkat awal (IS) radiasi gelombang mikro utama. Hal ini dapat menunjukkan bahawa proses longsor elektron berkelakuan impulsif sebelum penyebaran pengalir terbentuk. Selanjutnya, tiga NBE dengan radiasi gelombang mikro yang berkaitan telah dipetakan di mana sudut azimut dan ketinggian dapat ditentukan. Peta membuktikan bahawa ketiga-tiga NBE adalah hasil pemecahan positif yang cepat di mana longsor elektron (gelombang mikro) merambat ke atas sementara pengalir positif bergerak ke bawah.

ACKNOWLEDGEMENTS

In the Name of Allah, the Most Gracious, the Most Merciful

First and foremost, Alhamdulillah Almighty for the blessing of health, wisdom and patience to pass all the difficulties during my PhD journey.

I would like to take this opportunity to express my gratitude towards my supervisor Professor Dr. Badrul Hisham Bin Ahmad and my co-supervisor Dr. Mohd Riduan bin Ahmad for all his virtues during my PhD study specially during the difficulties of collecting the data during the pandemic of COVID-19. Thanks, from my deep hart for opening his house as measurement area. Special thanks to Associate Professor Dr. Mohamad Zoinol Abidin Bin Abd Aziz from the Faculty of Electronics and Computer Engineering (FKEKK), Universiti Teknikal Malaysia Melaka (UTeM), Durian Tunggal, Melaka, Malaysia for his support and guidance throughout the projects and encouragement in completing this research studies and thesis.

My gratitude and applauses I would like to give to my laboratory mates Ayman M. Ibrahim, Malik H. Al-Taweel, Mustafa M. A-Saedi, Sulaiman, Ammar, Seah, Dinesh, Haziq, En. Sufian and En. Imran for accompanying, supporting and providing me a lot of assistance during my research studies.

TABLE OF CONTENTS

	PAGE
DECLARATION	
APPROVAL	
DEDICATION	
ABSTRACT	i
ABSTRAK	ii
ACKNOWLEDGEMENTS	iii
TABLE OF CONTENTS	iv
LIST OF TABLES	vi
LIST OF FIGURES	vii
LIST OF ABBREVIATIONS	xvii
LIST OF PUBLICATIONS	xx
CHAPTER	
1. INTRODUCTION	1
1.1 Introduction	1
1.2 Research background	1
1.3 Problem statements	5
1.4 Research objectives	6
1.5 Scopes of research	7
1.6 Contribution of research work	8
1.7 Thesis organization	9
2. LITERATURE REVIEW	11
2.1 Introduction	11
2.2 Formation of thunderclouds	11
2.3 Lightning initiation mechanism	15
2.4 Types of lightning flashes and their corresponding waveforms	19
2.4.1 Intra-cloud flash (IC)	20
2.4.2 Narrow bipolar event (NBE)	26
2.4.3 Ground flashes	28
2.5 Sign convention and the relationships with Maxwell's equations	32
2.6 The mechanism of electromagnetic field detection	33
2.7 Historical development Microwave of radiations emitted by lightning flashes	39
2.8 Fast breakdown mechanisms and narrow bipolar event (NBE)	51
2.9 Lightning mapping	53
2.9.1 Magnetic field direction finding (MDF)	55
2.9.2 Time of arrival (TOA)	56
2.9.3 Interferometry	59
2.10 Low noise amplifier (LNA)	73
2.10.1 Biasing network	76
2.10.2 Stability condition	76
2.10.3 Noise figure	77
2.10.4 Power, transducer, available power gain	78
2.11 Band pass filter (BPF)	80
2.12 Fast antenna system	85

2.13	Critical review	86
2.13	Summary	89
3.	METHODOLOGY	90
3.1	Introduction	90
3.2	General flow of research	90
3.3	Flow of the design and development of lightning measurement system	92
3.4	Experimental setup and instrumentation	98
3.5	Microwave interferometer system	100
3.6	Simulation, fabrication and calibration of parallel plate antennas	103
3.7	Simulation, fabrication and calibration of low noise amplifier LNA	109
	3.7.1 Transistor type selection	109
	3.7.2 Low noise amplifier (LNA) design technique	110
3.8	Simulation, fabrication and calibration of band pass filter (BPF)	112
	3.8.1 Band pass filter (BPF) design	113
3.9	Simulation, fabrication and calibration of buffer circuit	117
3.10	Interferometer mapping technique	125
3.11	Time synchronization between LD and interferometer systems	127
3.12	Identification of flash types (NBEs) and method of analysis for microwave characterizations	128
3.13	Summary	136
4.	RESULT AND DISCUSSION	137
4.1	Introduction	137
4.2	Interferometer system development	137
	4.2.1 Simulation and calibration results of finite antenna	137
	4.2.2 Simulation and calibration results of low noise amplifier	143
	4.2.3 Simulation and calibration results of band pass filter	146
4.3	Temporal characteristic and interferometer mapping	149
	4.3.1 Temporal characteristic of narrow bipolar event	149
	4.3.2 Temporal characteristic of microwave radiation	159
	4.3.3 Microwave interferometer mapping	164
4.4	Discussion	166
	4.4.1 Comparison between temporal analysis of NBE and previous studies	166
	4.4.2 Temporal analysis of microwave radiation	167
	4.4.3 Comparison between microwave radiations detected at various distances	168
	4.4.4 Comparison between onset time of microwave and NBE	168
	4.4.5 Relationship between fast breakdown mechanism and NBEs	169
4.5	Summary	170
5.	CONCLUSION AND FUTURE WORKS	171
5.1	Conclusion	171
5.2	Future works and recommendations	172
	REFERENCES	174

LIST OF TABLES

TABLE	TITLE	PAGE
2.1	Temporal characteristics of the lightning processes in CG flash (Cooray, 2015)	30
2.2	Summary of the microwave radiation emitted by lightning flashes	49
2.3	Statistical data of positive narrow bipolar events (radiation) of previous studies	53
2.4	Summary of related work on interferometer	69
3.1	Specification of LeCroy wavesurfer 3054 oscilloscope	102
3.2	Parameter's list of the antenna	107
3.3	List of components for designing buffer circuit	118
4.1	Parameter's list and value of the LNA designed in ADS	145
4.2	Fabricated parameters result of the LNA	145
4.3	Parameter's list and value of the BPF designed in ADS	147
4.4	Fabricated parameters result of the BPF	148
4.5	Selected lightning flashes detected scheduled as type, date and time (Malaysia local time)	151

LIST OF FIGURES

TABLE	TITLE	PAGE
1.1	Cloud tripolar structure (Dwyer and Uman, 2014)	2
1.2	Types of cloud to ground flashes (CG) (a) Negative cloud to ground flash (-CG) (b) Positive cloud to ground flash (+CG). Assigned by using atmospheric sign convention	3
1.3	Types of narrow bipolar events flashes (a) Positive narrow bipolar event (b) Negative narrow bipolar event. Based on atmospheric sign convention	4
2.1	Types of clouds (a) Cumulus (b) Cumulus congestus (c) Cumulonimbus. Photographs courtesy national oceanic and atmospheric administration (NOAA), USA (Cooray, 2015)	12
2.2	Tripole charged structure of thundercloud. Different temperature at different altitude would affect the behaviour of graupels inside cumulonimbus nimbus and eventually turned out to be a thundercloud with tripole charged structure. IC and -CG flashes are the common lightning flashes that occur in our daily life followed by +CG flash (Rakov 2007)	14
2.3	Townsend electron avalanche visualisation. Note that the liberated electron (red dot) will continue colliding with another air molecule to	17

	liberate another new electron (new red dot) while the former electron is now indicated by the black dot (Seah, 2020)	
2.4	Example of mechanism (a) Positive streamer and (b) Negative streamer (Cooray, 2015)	19
2.5	An example of IC pulses train E-field waveform. Window (i) and (ii) are the extended views of window (a) which shows an example of IC pulses (Seah 2020)	24
2.6	An example of +NBE E-field radiation. Note that window (i) is the extended view of window (a) (Seah 2020)	25
2.7	An example of -NBE captured with its static component. Window (a) is the original waveform captured while window (i) is the zoomed in version of window (a) (Seah 2020)	26
2.8	Example of positive narrow bipolar event (+NBE) (Ahmad et al., 2014)	27
2.9	Example of Negative narrow bipolar event (-NBE) (Ahmad et al., 2014)	27
2.10	Example of a full process for a -CG flash captured (2 s time frame) from Malaysia thunderstorm in May 2016 (Seah 2020)	30
2.11	A basic -CG process which consists of IB, SL and RS. Window (a) is the zoomed in version of Figure 2.10. Window (i) shows the extended view of IB pulses train while window (ii) is the SL and -RS process (Seah 2020)	31
2.12	Example on how the capacitive antenna receive the signal produced by lightning flash	34
2.13	Electric field mills system	35

2.14	Operation of electric field mills under different background electrostatic field. Note that (a) and (b) are under the condition where the area is affected by the main negative charge region of the thundercloud while (i) and (ii) are the condition whereby the thundercloud is right on top of the electric field mills (affected by small positive pocket charge of the thundercloud)	35
2.15	Diagram of charge displaced from the sphere and direction of electric field (Cooray, 2015)	38
2.16	Schematic diagram for the setup of measurement (Brook and Kitagawa, 1964)	40
2.17	Schematic of measurement set-up by Kosarev research group (Kosarev et al, 1970)	41
2.18	Schematic diagram of the measurement setup (Rust et al, 1979)	42
2.19	Schematic diagram of the measurement setup by Le Boulch et al. The dotted lines indicate triggering signals (Le Boulch et al., 1987)	43
2.20	Block diagram of the radiometer used by Fedorov et al. Note that (f) represents fine channel while (c) represents coarse channel; e.g. PD (f) and PD (c) are the peak detectors of the fine and coarse channels (Fedorov et al., 2001)	44
2.21	Diagram of measuring site (Yoshida, 2008)	45
2.22	Diagram for setup of lightning remote sensing system (Ahmad et al., 2013)	46
2.23	Schematic diagram for apparatus setup (Peterson and Beasley, 2013)	47

2.24	NBE producing storm by observation of lightning mapping array LMA (Rison et al., 2016)	51
2.25	Orthogonal magnetic antenna	55
2.26	Basic architecture of interferometer (Stock et al., 2014)	59
2.27	First published interferometric observation of lightning (Warwick et al. 1979)	60
2.28	First published 2-D interferometric map of lightning (Hayenga and Warwick 1981)	61
2.29	NMT narrowband interferometer map of a lightning discharge (Shao and Krehbiel, 1996)	63
2.30	Simple block diagram of low noise amplifier (Al-Shaikhli et al., 2017)	74
2.31	Band pass filter response (Chen et al. 2009)	81
2.32	Return loss response of the band pass filter (Kircay et al. 2009)	82
2.33	Return loss response for narrow band pass filter (Zahradnik and Vlcek, 2004)	84
2.34	The fast antenna system consists of parallel plate antenna, buffer circuit, and digitizer (Ahmad et al. 2013)	86
3.1	General flow of the research work	91
3.2	Schematic of the measurement setup	93
3.3	Process flow of constructing fast electric field sensor for lightning remote sensing system	94
3.4	Process flow of constructing microwave antenna electric field sensor	95
3.5	Process flow of constructing low noise amplifier (LNA)	96
3.6	Process flow of constructing band pass. Filter (BPF)	97

3.7	Block diagram for interferometer lightning remote sensing measurement setup	99
3.8	Measurement site located at Paya Rumpit, Melaka, Malaysia	99
3.9	Structure of the interferometer system with FA system	100
3.10	The combination of microwave radio system (LNA with BPF) and its measurement results by vector network analyzer (VNA)	101
3.11	Installation of parallel circular antenna for FA record sensor system	103
3.12	Simulation design of parallel plate antenna with distance of 16 mm air gap using CST software simulation	105
3.13	Simulation results of the electric field flows in 3D forms	105
3.14	Example of the direction of electric field is downwards vertically	106
3.15	Antenna design structure of A3 finite antenna in CST (a) Structure of top plate (b) Structure of ground plate (c) Separation between two plates (air gap) (d) Overview of the finite antenna designed (Note that yellow region is copper patch while white region is FR-4 substrate)	106
3.16	Example of one of the fabricated antennas for microwave sensing purposes (a) Side view (b) Top view (c) Bottom view	108
3.17	The calibration of the antenna under far-field measurement in anechoic chamber	109
3.18	Design structure for S-parameter technique	110
3.19	Schematic design of low noise amplifier LNA by using ADS software	111
3.20	Fabricated low noise amplifier using FR-4	112

3.21	Calibrated and measurement of LNA using vector network analyser (VNA)	112
3.22	Parallel series type topology of 8th order band pass filter (BPF)	114
3.23	Design schematic lumped elements of 8th order band pass filter by using ADS	114
3.24	Momentum schematic for the band pass filter By ADS	115
3.25	Fabricated band pass filter (BPF) by using FR-4 substrate with SMA ports feeding	116
3.26	BPF measuring by using vector network analyser (VNA)	116
3.27	Designing buffer circuit for fast E-field using Multisim software	119
3.28	Ultraviolet (UV) expose machine	120
3.29	Etching and cutting circuit board	120
3.30	Drilling the holes for fitting in the components and soldering them	120
3.31	Flow of the fabrication process PCB board	121
3.32	Design of buffer circuit for fast E-field (a) Schematic layout designed by using ARES software (b) Example of fabricated circuit (PCB) board (c) Example of buffer circuit	122
3.33	Example of coaxial cable, RG-58 being calibrated (left-hand-side was the calibration when both positive and negative probes contacted the core of RG-58 while right-hand-side was the calibration when one of the probes touched the BNC cover)	122
3.34	Flow of the troubleshooting and continuity check on coaxial cable	123
3.35	Calibrating the buffer circuit by using LeCroy Wavesurfer 3054 oscilloscope	124

3.36	Example of calibrating results of buffer circuit. Note that the output signal (pink colour) is overlapping with the input signal (yellow colour)	124
3.37	An example of PPS signal captured together with fa record	127
3.38	Example of NBE waveform compared to its corresponding radiation pattern (dotted line) (Eack, 2014)	128
3.39	Example +NBE with its associated microwaves emissions captured at 16:07:40 (+8 UTC), 21 May 2020	129
3.40	Zoomed in version of FA record from Figure 3.39	129
3.41	Overview of the main burst of microwave radiation and its basic parameters in characterization process from Figure 3.39	130
3.42	Overview of IS of microwave main burst in Figure 3.41	130
3.43	Example of the FA record produced by -NBE and its basic parameters in characterization process captured at 16:22:47 (+8 UTC), 21 May 2020	131
3.44	Example of -NBE (radiation) with its associated microwave emissions captured at 16:22:47 (+8 UTC), 21 May 2020	132
3.45	Parameters measured for each emission in the characterization of -NBE (radiation)	133
3.46	Example NBE (radiation) with its associated microwave emissions captured at 05:12:24 (+8 UTC), 25 May 2020	130
3.47	Example of the FA record produced by +NBE (radiation) and its basic parameters in characterization process	135
3.48	Example of the microwave produced by +NBE (radiation) and its basic parameters in characterization process	135

4.1	Return loss $S_{1,1}$ simulation results of the finite antenna across different height of air gap (a) The $S_{1,1}$ value when d changeable from 12 mm to 19 mm air gap (b) The $S_{1,1}$ value when d equal to 16 mm	139
4.2	Simulation results of radiation pattern of the finite antenna at 0.9978 GHz (a) shows the 3D view while (b) presents the simulation of polar plot of the radiation pattern obtained	140
4.3	Return loss $S_{1,1}$ of parallel plate A3 finite antenna measured by VNA	141
4.4	Simulation and measured results for return loss $S_{1,1}$ of parallel plate A3 antenna	141
4.5	Measurement and calibration of parallel A3 finite antenna	142
4.6	Radiation patterns of finite antenna in far field measurement at 0.994 GHz	143
4.7	Gain $S_{2,1}$, return loss $S_{1,1}$ and noise figure (NF) simulation results parameters of LNA using ADS	146
4.8	Gain $S_{2,1}$ and return loss $S_{1,1}$ fabrication results of the LNA measured by VNA	146
4.9	Return loss $S_{1,1}$ and $S_{2,1}$ simulation results parameters of BPF using ADS	147
4.10	Return loss $S_{1,1}$ and $S_{2,1}$ fabrication results of the LNA measured by VNA	144
4.11	Temporal characteristics of +NBEs	150
4.12	The distance between microwave interferometer system and LD station located in UTeM	150

- 4.13 Lightning strikes captured by LD system on 21 May 2020, +8 UTC 152
 16:00 – 17:00 (a) Lightning strikes that captured by LD system (b)
 EMF record in 2 hours (c) Total number of the strikes captured by LD
 system within 100 km radius (d) Total number of the strikes captured
 respective to their distance from our systems
- 4.14 Lightning strikes captured by LD system on 22 May 2020, +8 UTC 153
 15:00 – 16:00 (a) Lightning strikes that captured by LD system. (b)
 EMF record in 2 hours (c) Total number of the strikes captured by LD
 system within 100 km radius (d) Total number of the strikes captured
 respective to their distance from our systems
- 4.15 Lightning strikes captured by LD system on 25 May 2020, +8 UTC 154
 05:00 – 06:00 (a) Lightning strikes that captured by LD system (b)
 EMF record in 2 hours (c) Total number of the strikes captured by LD
 system within 100 km radius (d) Total number of the strikes captured
 respective to their distance from our systems
- 4.16 Lightning strikes captured by LD system on 26 May 2020, +8 UTC 155
 04:00 – 05:00 (a) Lightning strikes that captured by LD system (b)
 EMF record in 2 hours (c) Total number of the strikes captured by LD
 system within 100 km radius (d) Total number of the strikes captured
 respective to their distance from our systems
- 4.17 Lightning strikes captured by LD system on 26 May 2020, +8 UTC 157
 13:00 – 14:00 (a) Lightning strikes that captured by LD system (b)
 EMF record in 2 hours (c) Total number of the strikes captured by LD

	system within 100 km radius (d) Total number of the strikes captured respective to their distance from our systems	
4.18	Locations of NBEs Captured by LD System on 21 May 2020, UTC+8 16:00 to 17:00.	157
4.19	Locations of NBEs Captured by LD System on 22 May 2020, UTC+8 between 15:33:37 and 16:31:23	157
4.20	Locations of NBEs Captured by LD System on 25 May 2020, UTC+8 05:12:20	158
4.21	Locations of NBEs Captured by LD System on 26 May 2020, UTC+8 04:15:28 and 13:40:08	158
4.22	Distribution of the number of initial stage (IS) of microwave radiation samples for each channels B, C, and D	159
4.23	Distribution of number of individual pulses during IS stage	159
4.24	Temporal characteristics of individual microwave bipolar pulses duration within IS for all channels	161
4.25	Temporal characteristic of total duration of IS	161
4.26	Temporal characteristics of microwave main bursts that associated with NBEs presents the value of rising phase (RP)	162
4.27	Temporal characteristics of microwave main bursts that associated with NBEs presents the value of damping phase (DP)	162
4.28	Temporal characteristics of microwave main bursts that associated with NBEs presents the value of total pulse train duration (TPTD)	163

- 4.29 Distribution of onset time of microwave relative to onset of NBEs. note 164
that top column represents the leading samples, and the bottom column
represents lagging samples
- 4.30 Microwave interferometer mapping for +NBE2 with clear almost 165
vertical channel and clear channel propagation. yellow and green
circles are the microwave impulsive locations (Azimuth, Elevation),
the red waveform is NBE, and the grey burst is microwave burst
- 4.31 Microwave interferometer mapping for +NBE10 with clear almost 165
vertical channel and clear channel propagation. yellow and green
circles are the microwave impulsive locations (Azimuth, Elevation),
the red waveform is NBE, and the grey burst is microwave burst
- 4.32 Microwave interferometer mapping for +NBE11 with clear almost 166
vertical channel and clear channel propagation. yellow and green
circles are the microwave impulsive locations (Azimuth, Elevation),
the red waveform is NBE, and the grey burst is microwave burst

LIST OF ABBREVIATIONS

ADS	-	Advanced Design System
BNC	-	Bayonet Neill–Concelman
BPF	-	Band Pass Filter
CAPPI	-	Constant Altitude Plan Position Indicator
CID	-	Compact Intra-cloud Discharge
CG	-	Cloud-to-Ground
CPT	-	Chaotic Pulse Train
CST	-	Computer Simulation Technology
dB/dt	-	Time derivative magnetic field
dE/dt	-	Time derivative electric field
DP	-	Damping Phase
FA	-	Fast electric field Antenna
FB	-	Fast Breakdown
FNB	-	Fast Negative Breakdown
FPB	-	Fast Positive Breakdown
FR4	-	Flame Retardant 4
IB	-	Initial Breakdown
IC	-	Intra-Cloud
IS	-	Initial Stage
LD	-	Lightning Detector
LF	-	Low Frequency
LMA	-	Lightning Mapping Array
LNA	-	Low Noise Amplifier

MDF	-	Magnetic Direction Finder
MMD	-	Malaysia Meteorological Department
NBE	-	Narrow Bipolar Event
PCB	-	Printed Circuit Board
PD	-	Pulse Duration
PTD	-	Pulse Train Duration
RT	-	Rise Time
RP	-	Raising Phase
SMA	-	Sub Miniature version A
TOA	-	Time of Arrival
TPTD	-	Total Pulse Train Duration
UHF	-	Ultra High Frequency
VHF	-	Very High Frequency
VLf	-	Very Low Frequency
ZCT	-	Zero-Crossing Time
+CG	-	Positive Cloud-to-Ground
+NBE	-	Positive Narrow Bipolar Event
-CG	-	Negative Cloud-to-Ground
-NBE	-	Negative Narrow Bipolar Event

